



Removal of Lead (II) by Lumbang, *Aleurites moluccana* Activated Carbon Carboxymethylcellulose Composite Crosslinked with Epichlorohydrin

NELSON R. VILLARANTE¹, RONNETTE ANNE E. DAVILA¹ and DERICK ERL P. SUMALAPAO^{2,3,*}

¹Department of Physical Sciences and Mathematics, College of Arts and Sciences, University of the Philippines Manila, Manila, Philippines.

²Department of Biology, College of Science, De La Salle University, Manila, Philippines.

³Department of Medical Microbiology, College of Public Health, University of the Philippines Manila, Manila, Philippines.

*Corresponding author E-mail: derick.sumalapao@dlsu.edu.ph

<http://dx.doi.org/10.13005/ojc/340211>

(Received: November 05, 2017; Accepted: January 01, 2018)

ABSTRACT

Removal of Pb(II) using lumbang activated carbon carboxymethylcellulose composite crosslinked with epichlorohydrin was investigated. Batch adsorption studies were performed to evaluate the effects of pH, contact time, temperature, adsorbent dose, and metal concentration. To characterize the adsorbent, proximate analysis, bulk density, DSC, FT-IR, and SEM analysis were performed. Results of FT-IR revealed that crosslinking did not alter the structure of carboxymethylcellulose due to the presence of the $-\text{COO}$ functional groups, while the presence of the C-O signal indicates that the adsorbent was successfully crosslinked by epichlorohydrin. Furthermore, SEM results showed highly porous nature of the prepared adsorbent. The optimized parameters of the adsorbent were pH 3, contact time of 15 min. 30 °C temperature, adsorbent dose of 4 g/L at 5 ppm Pb (II) solution. With these optimized parameters, 73% removal of Pb (II) was attained in aqueous solutions, while 37% removal was observed in the wastewater sample. Moreover, the adsorption process was best described by Dubinin-Radushkevich isotherm and obeyed the pseudo-second order kinetic model.


Keywords: Biosorption, Pb(II), Lumbang, *Aleurites moluccana*, Activated carbon carboxymethylcellulose, Epichlorohydrin crosslinking.

INTRODUCTION

The presence of heavy metals in different water sources poses danger in aquatic ecosystems and risks in human health. One of these heavy

metals is Pb(II), a naturally occurring, toxic, and commercially useful metal^{1,2}. To meet these problems of heavy metal contamination in water, adsorbents were developed. One of the conventional adsorbents used is activated carbon



This is an  Open Access article licensed under a Creative Commons Attribution-NonCommercial-ShareAlike 4.0 International License (<https://creativecommons.org/licenses/by-nc-sa/4.0/>), which permits unrestricted NonCommercial use, distribution and reproduction in any medium, provided the original work is properly cited.

(AC) due to its large adsorption capacity, rapid adsorption kinetics, and relative ease of regeneration^{3,4}. However, commercially available activated carbon is expensive, and production of this adsorbent from agricultural wastes emerged as a reasonable alternative. Activated carbon can be obtained from materials with high carbon content⁵. The nature of the precursor and the methods performed in the production of activated carbon affects the final adsorption properties of the adsorbent⁶. Due to the developing trend in the production of activated carbon from cheaper raw materials and from renewable biomass, the conversion of various environmental wastes such as coconut shells⁷, tamarind wood⁸, snail shell waste⁹, pine cones², and hazelnut husks¹⁰ to activated carbon were already successfully investigated. Moreover, activated carbon is usually coated with compounds to further enhance its adsorption capacity¹¹. In addition to activated carbon, carboxymethylcellulose (CMC) which is an ionic polysaccharide containing carboxyl groups is also used for heavy metal adsorption. CMC-derived adsorbents are cheap, abundant, and biodegradable, a good starting material for adsorbent preparation¹². To improve the physical and chemical properties of carboxymethylcellulose, it is usually crosslinked with epichlorohydrin (ECH), a colorless liquid and moderately soluble in water, but miscible with most polar substances¹³.

In this paper, novel synthesis of low-cost lumbang, *Aleurites moluccana* activated carbon carboxymethylcellulose composite crosslinked with epichlorohydrin (LAC/CMC/ECH) by irradiation was performed and its adsorption capacity using Pb(II) in aqueous medium and wastewater sample was evaluated. A microcosm adsorption study of LAC/CMC/ECH hydrogel composite on Pb (II) removal as a function of pH, temperature, contact time, initial concentration of adsorbate, and adsorbent dose was investigated. The physicochemical characterization of the composite was limited to proximate analysis and bulk density, differential scanning calorimetry (DSC), Fourier transform infrared (FT-IR) spectroscopy, and scanning electron microscopy (SEM). Moreover, adsorption kinetics and isotherm studies were also done to assess the possible mechanism of interaction. The LAC/CMC/ECH composite is useful

for the general remediation of wastewater generated from industries and laboratories, especially those that contain large amount of Pb (II) as treatment of these contaminated water may reduce toxicity in aquatic ecosystems.

MATERIALS AND METHODS

Reagents and plant material

Lumbang, *Aleurites moluccana* seed shells were collected from the College of Forestry, University of the Philippines, Los Banos, while the wastewater samples were collected from Pasig River in Sta. Cruz, Manila, Philippines. Sodium carboxymethylcellulose (MWt: ~250,000) and (\pm) epichlorohydrin were purchased from Sigma-Aldrich. Lead nitrate (99.9% purity, Merck Chemicals) was used for the preparation of the Pb (II) aqueous medium. Electron beam irradiation was performed at the Irradiation Facility at Philippine Nuclear Research Institute (PNRI).

Preparation of the charcoal

To prepare lumbang activated carbon (LAC), dry lumbang seed shells were crushed, dried, and washed with water to remove impurities before subjecting to a traditional pyrolytic burrow method. A shallow burrow was made wherein the shells were incinerated for 5 h, with the soil as cover to prevent entry of oxygen. Afterwards, the charcoal was washed with deionized water, sorted to a particle size ranging from 0.149-0.250 mm, and washed with deionized water.

Activation of the charcoal

In the activation process, CaCl_2 was used as the activating agent⁷. The collected charcoal was pulverized and was soaked in 25% CaCl_2 solution for 24 h, washed five times with deionized water, and oven-dried at 100 °C.

Preparation of the composite

To prepare 20 wt.% CMC and 5 wt.% LAC, 20 g of CMC and 5 g of LAC with 5 g of NaOH in deionized water were mixed^{14,15}. Afterwards, 10 mL of ECH was added to the 90 mL of CMC solutions, and was mixed thoroughly. The resulting mixture was sent to the irradiation facility at PNRI and was irradiated by electron beam at 25 kGy to facilitate crosslinking. The irradiated adsorbent was

oven-dried at 50 °C for 16 h, pulverized, washed with deionized water, and sorted using a 40-60 mesh sieve to obtain a uniform size of 0.420-0.814 microns.

Characterization of the composite bulk density (BD)

A certain amount of adsorbent was placed inside a 10-mL graduated cylinder up to a specified volume. The weight of the adsorbent was measured and the bulk density was calculated using the equation

$$\text{Bulk Density} = \frac{\text{weight of dried adsorbent (g)}}{\text{volume of packed dried material (cm}^3\text{)}}$$

Proximate analysis

Proximate analysis includes the analysis of moisture, ash, crude fat, crude fiber, and crude protein contents. Samples were sent to the Biotech Central Analysis Laboratory, University of the Philippines, Los Banos, Philippines.

Differential scanning calorimetry

Differential scanning calorimetry (DSC) analysis was conducted for the composites on a Perkin-Elmer DSC 4000 apparatus under N₂ flow with the samples hermetically sealed in aluminum pans.

Scanning electron microscopy

Samples of the composite before and after adsorption were sent to the Surface Morphology Laboratory, De La Salle University, Philippines for SEM analysis using a JSM-5310 scanning microscope.

FT-IR spectroscopy

The FT-IR spectra were recorded at room temperature in the range of 4000–500 cm⁻¹ on a ThermoScientific Nicolet 6700 FT-IR spectrometer using a KBr pellet sampling method and were accumulated for 16 scans.

Adsorption experiments

Adsorption experiments were done by batch studies in 15 mL conical tubes by soaking the dried composite in 5 mL of aqueous Pb (II) solutions, and agitating this using SHZ-82A water bath shaker at 156 rpm. Pb (II) determination was done using AAS (Shimadzu AA-6300). Adsorption

study as function of pH, contact time, temperature, adsorbent dosage, and initial Pb (II) concentration was conducted.

Effect of pH

Batch studies at different pH (2-7) were conducted by soaking the adsorbent in 10 ppm of Pb (II) in each microcosm. Each container was agitated (156 rpm) for 1 h at 30 °C.

Effect of contact time

Optimum contact time was determined by soaking the adsorbent in 10 ppm of Pb (II) ions. Each microcosm was prepared at 30 °C and pH 3. The rate of adsorption was monitored every 15 min. for a period of 2 hours.

Effect of temperature

The same preparation was made, except for the varying temperature conditions. The microcosm which was maintained at pH 3 was incubated at different temperatures 20-40 °C for a period of 15 minutes.

Effect of adsorbent dosage

Microcosms with different adsorbent doses (1-7 g/L) were amended with 10 ppm of Pb (II) in aqueous solutions. The rate of adsorption was monitored at the following optimum conditions: pH of 3, 30 °C temperature, 15 min. contact time.

Effect of Pb (II) concentration

The composite was soaked in 5, 10, 20, 30, 40, 50, 60, and 70 ppm aqueous solutions of Pb (II) at the optimum pH, contact time, temperature, and adsorbent dose.

Adsorption isotherms

Adsorption isotherms represent the relationship of the amount of metal adsorbed with the adsorbent dose. These provide information about the mechanism of adsorption and the adsorptivity of the composite towards the metal of interest¹⁶. In this study, Langmuir, Freundlich, Temkin, and the Dubinin-Radushkevich isotherms were investigated.

Langmuir isotherm

Monolayer adsorption onto the surface of the adsorbent is assumed by the Langmuir

isotherm. In this model, it is assumed that binding of metals onto the adsorbent is homogeneous, and that adsorption will no longer take place once equilibrium has been established. Also, this model predicts an equal distribution of metal ions between the liquid and solid phases¹⁷. The linear form of the Langmuir isotherm is described by

$$\frac{1}{q_e} = \frac{1}{Q_0} + \frac{1}{Q_0(K_L)} \frac{1}{C_e}$$

where q_e is the amount of metal adsorbed per gram of the adsorbent (mg/g), C_e is the maximum monolayer capacity (mg/g), Q_0 is the maximum monolayer coverage capacity (mg/g), and K_L is the Langmuir isotherm constant.

Freundlich isotherm

The Freundlich isotherm is an empirical equation used to model multilayer adsorption on heterogeneous adsorbents, with the assumption that sites of adsorption exponentially increase with an increase in the heat of absorption¹⁸. This can be expressed mathematically as

$$\ln q_e = \ln K_f + \frac{1}{n} \ln C_e$$

where q_e is the amount of metal adsorbed per gram of the adsorbent (mg/g), C_e is the equilibrium concentration of the adsorbate (mg/L), n is the adsorption intensity, and K_f is the Freundlich isotherm constant.

Temkin isotherm

The Temkin isotherm considers the adsorbent-adsorbate interactions, with the assumption that the heat of adsorption of the molecules in the layer would exhibit a linear, instead of a logarithmic, decrease¹⁷. This relationship is described by

$$q_e = B \ln A_T + B \ln C_e$$

where q_e is the amount of metal adsorbed per gram of the adsorbent (mg/g), C_e is the equilibrium concentration of the adsorbate (mg/L), A_T is the equilibrium binding constant, and B is the heat of sorption constant.

Dubinin-Radushkevich isotherm

The Dubinin-Radushkevich isotherm (D-R isotherm) predicts whether the mechanism of adsorption is physical or chemical. It is also useful for the estimation of the porosity and the free energy of adsorption. The D-R isotherm is a more general form of the Langmuir isotherm¹⁹. The linear form of the D-R isotherm is expressed as

$$\ln q_e = \ln q_s - K_{ad} \varepsilon^2$$

where q_e is the amount of metal adsorbed per gram of the adsorbent (mg/g), q_s is the theoretical isotherm saturation capacity, K_{ad} is the Dubinin-Radushkevich isotherm constant (mol^2/J^2), and ε is the mean adsorption energy.

Adsorption kinetics

Adsorption kinetic studies were performed using the first order, second order, pseudo-second order, and the Elovich models^{20,21}.

Wastewater analysis and efficiency experiment

Under optimized conditions, the dried adsorbent was soaked in wastewater samples obtained from Pasig River, Sta. Cruz, Manila, Philippines. First, the wastewater sample was filtered before the adsorption study was conducted, and then was subjected to acid digestion using concentrated HNO_3 by heating 50 mL of the sample to 80 °C, followed by the addition of 15 mL HNO_3 , before atomic absorption spectrophotometer (AAS) analysis²². Other metals present in wastewater like cadmium and magnesium were also determined but were not subjected to adsorption study.

Following the optimized parameters, the adsorption ability of the adsorbent was tested in an organic compound, methylene blue²³. The adsorption abilities of commercial AC, LAC, CMC, LAC/CMC, and LAC/CMC/ECH were also tested in aqueous solutions of Pb (II) using the optimized parameters.

RESULTS AND DISCUSSION

Adsorbent characterization

Bulk density, Moisture content, and Proximate analysis

The bulk density, moisture content, and proximate analysis of the adsorbent were

determined (Table 1). Bulk density is the ratio of the mass of the pulverized adsorbent with the volume, and it is indicative of porosity. It is dependent on the density of the adsorbent, as well as on its arrangement in space. Based from the result, 0.56 g of adsorbent occupies 1 cm³. A bulk density greater than 0.4 indicates that the adsorbent is highly porous²⁴, this means that the prepared adsorbent is highly porous. Moisture content is the amount of water in the sample that causes variations in the weight, density, and viscosity of the adsorbent, while ash content is defined as the mineral matter, such as clay or silica, present in the raw material that may alter the pore development of the composite. Ash content may be acquired from the environment as a contaminant during the collection of raw materials. Therefore, lower ash content equates to a better pore structure. Crude fat refers to the fat-soluble material present in the sample, while crude fiber refers to the amount of indigestible cellulose, and lastly, crude protein content refers to the total nitrogen content of the sample. Based on the proximate analysis results (Table 1), the protocol employed in the production of charcoal is effective due to the low ash content and moisture content.

Table 1: Bulk density, moisture content, and proximate analysis of the adsorbent

Bulk Density (g/mL)	0.56
Moisture Content (%)	5.07
Ash Content (%)	1.67
Crude Fat (%)	3.51
Crude Fiber (%)	72.43
Crude Protein Content (%)	1.81

Differential scanning calorimetry

The DSC profile of the LAC/CMC/ECH composite was investigated (Fig. 1). The peak at 70.95 °C with a $\Delta H = 540.05$ J/g is the endothermic peak for the loss of water. At this point, the material undergoes a phase change from solid to liquid²⁵. On the other hand, the peak at 304.68 °C denotes the disintegration of the composite.

FT-IR spectroscopy

The adsorption peaks of the carboxylate group of CMC at 1600 cm⁻¹ (asymmetric stretching vibration) and 1453 cm⁻¹ (symmetric stretching

vibration) in both spectra were observed in the FT-IR spectra overlay of LAC/CMC and LAC/CMC/ECH composites (Fig. 2). The bands at 3400 cm⁻¹ and 2900 cm⁻¹ were due to stretching vibration of -OH and C-H, respectively. The peak at around 1062 cm⁻¹ is a typical stretching frequency of the ether group of the polysaccharide while the medium peak at around 1328 cm⁻¹ can be attributed to the C-O stretch of the carboxylate. The medium ring deformation band observed at 871 cm⁻¹ in the LAC/CMC/ECH composite is due to the presence of the ECH, and is not observed in LAC/CMC composite. Furthermore, the peak at around 1421 cm⁻¹ in LAC/CMC was shifted to 1452 cm⁻¹ in LAC/CMC/ECH with the appearance of peak at around 871 cm⁻¹ which is possibly attributed to the formation of intramolecular hydrogen bonding that would occur between the -OH of ECH and neighboring oxygen of the CMC and AC. Moreover, there is a change in the spectral profile of the composite before and after adsorption of Pb (II) ion (Fig. 3). There is a decrease in the intensity around 1452 cm⁻¹ and the disappearance of C-O-C bending vibration of the ECH at around 871 cm⁻¹ possibly reflecting the interaction with Pb (II) through complexation reaction. A new broad peak was also observed at around 2180 cm⁻¹ after adsorption of Pb (II) ion.

Scanning electron microscopy

Scanning electron micrographs of LAC and LAC/CMC/ECH (before and after adsorption) composites were obtained using JSM-5310 scanning microscope (Fig. 4). There is an increase in porosity of the surface when a pure LAC (Fig. 4a-b) was crosslinked with CMC and ECH (Fig. 4c-d). Moreover, the surface morphology of the LAC/CMC/ECH after adsorption of Pb(II) ion is quite different (Fig. 4e-f) as the pores become circular and smaller after adsorption.

Adsorption experiment

Effect of pH

The effect of pH on Pb (II) adsorption on LAC/CMC/ECH composite (10 ppm Pb initial concentration, 5 g/L adsorbent dose, 60 min. contact time, 30 °C temperature, constant agitation) showed that the highest percent removal is at pH 3 (Fig. 5a). At lower pH, the carboxyl group is in the form -COOH due to the protonation of the carboxyl functional

groups present in the adsorbent. However, starting at pH 3, these carboxyl groups become carboxylate anions, binding Pb (II) ions through electrostatic interactions¹². Some studies have reported that adsorption between pH 3 to 5 produces the maximum percent removal. At lower pH, hydrogen ions will compete with the binding of Pb (II), whereas, at basic pH, precipitation of Pb (II) will take place. There is a negligible difference in the percent removal between pH 4 and 5, and there is an approximately 6% difference between the percent removal at pH 3. On the other hand, adsorption at pH 6 decreased and this may be attributed to the onset of Pb (II) precipitation. However, the gradual increase of uptake at pH 7 may be due to the complete deprotonation of the adsorbent²⁶.

Effect of contact time

The effect of contact time on Pb (II) adsorption on LAC/CMC/ECH composite (initial Pb concentration: 10 ppm, adsorbent dose: 5 g/L, pH: 3, temperature: 30 °C constant agitation) was examined (Fig. 5b). The percent removal values were compared across time intervals, there was no significant difference identified ($p>0.05$). In particular, a 65.15% removal was identified during the 15 min. and when compared to 63.60% removal during the 30 min., no significant difference was identified ($p>0.05$). Moreover, there is a negligible difference in the percent removal between time intervals which indicates that at an agitation rate of 156 rpm, the amount of Pb (II) removed is nearly constant for each time interval.

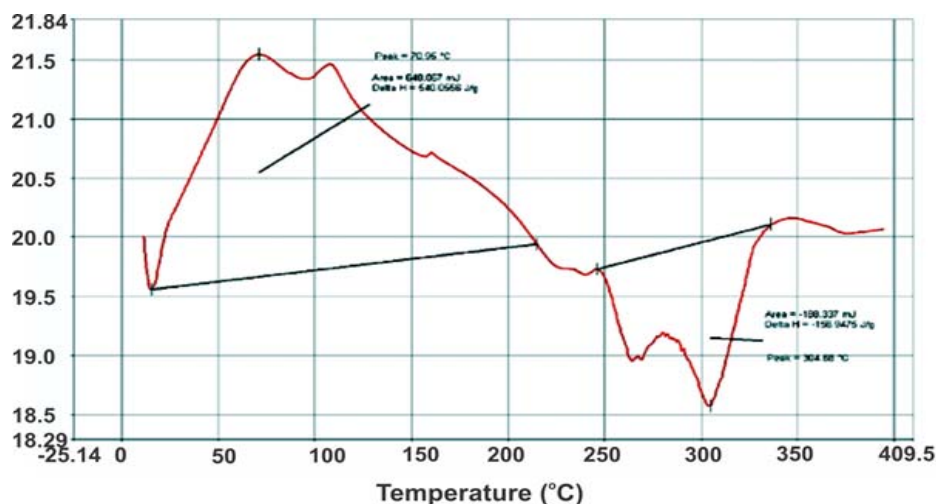


Fig. 1. Differential scanning calorimetry profile of the LAC/CMC/ECH composites

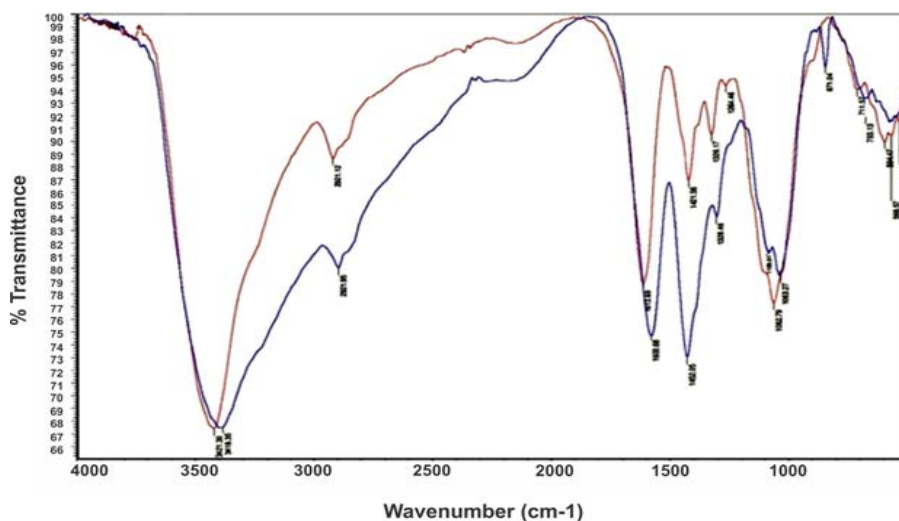


Fig. 2. Overlaid spectra of LAC/CMC (red) and LAC/CMC/ECH (blue) composites

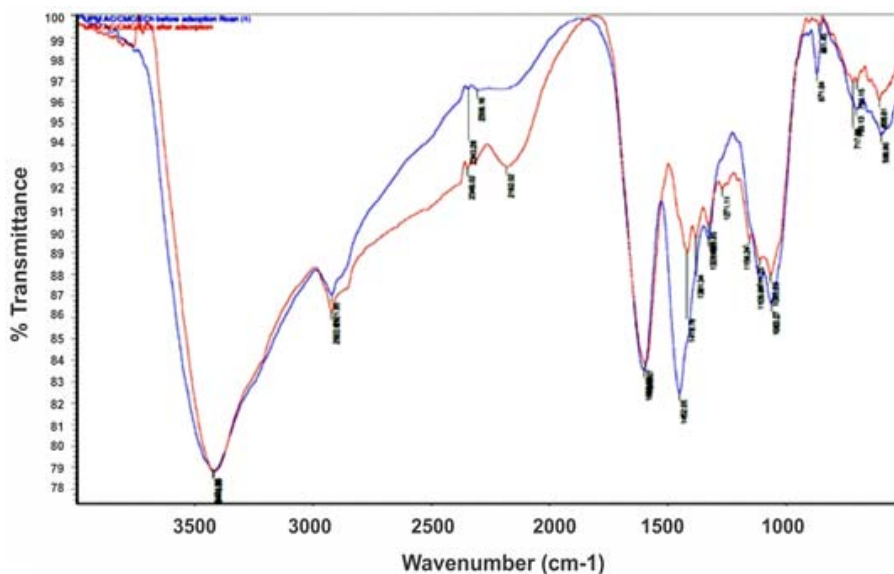


Fig. 3. Spectra of the LAC/CMC/ECH composite before (blue) and after (red) Pb(II) adsorption

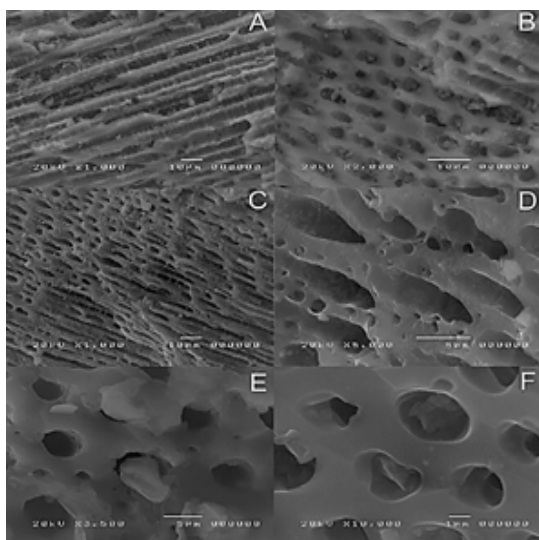


Fig. 4. SEM images of a) lumbang AC (x1000) b) lumbang AC (x2000) c) LAC/CMC/ECH composite - before adsorption (x1000) d) LAC/CMC/ECH composite - before adsorption (x5000) e) LAC/CMC/ECH composite - after adsorption (x3500) f) LAC/CMC/ECH composite - after adsorption (x10000)

Effect of temperature

The optimum temperature is at 30 °C when the effect of temperature on Pb (II) adsorption on LAC/CMC/ECH composite (initial Pb concentration: 10 ppm, adsorbent dose: 5 g/L, pH: 3, contact time: 15 min. constant agitation) was assessed (Fig. 5c). An increase in temperature

results to a decrease in percent removal since at higher temperature, the kinetic energy increases, facilitating desorption.

Effect of adsorbent dose

The effect of adsorbent dose on Pb (II) adsorption on LAC/CMC/ECH composite (initial Pb concentration: 10 ppm, temperature: 30 °C, pH: 3, contact time: 15 min. constant agitation) yielded an optimum adsorbent dose of 4 g/L (Fig. 5d). Lower doses adsorbed less Pb (II) since lower amount of the adsorbent has less adsorption sites^{20,21}. However, beyond 4 g/L there is a continuous decrease in the percent removal which means that the adsorptive capacity of the adsorbent was not highly utilized due to its aggregation. It is also possible that the increased amount of adsorbent resulted to overcrowding which can possibly lead to the overlapping of the adsorption sites²⁷.

Effect of metal concentration

The highest percent removal was seen at 5 ppm Pb (II) concentration when the effect of metal concentration on Pb (II) adsorption on LAC/CMC/ECH composite (adsorbent dose: 4 g/L, temperature: 30 °C, pH: 3, contact time: 15 min. constant agitation) was examined (Fig. 5e). It can also be observed that as the concentration of the metal increases, the percent removal decreases which reflects the limited number of adsorption sites in the composite and that at high concentrations, the adsorption sites become saturated^{20,21,28}.

Adsorption isotherms

The parameters and constants of the different isotherm models were calculated. Among these isotherm models, the D-R isotherm, with almost unity coefficient of determination (R^2), best describes the adsorption process (Table 2). The value of the mean free energy (E) of adsorption for the D-R isotherm indicates whether the adsorption

process is physisorption, an ion exchange, or a strong chemical adsorption. An E value less than 8 kJ/mol signifies physisorption, whereas between 8 and 16 kJ/mol suggests an ion exchange, and over 16 kJ/mol a stronger chemical adsorption than ion exchange^{29,30,31}. Hence, the adsorption process described in this study has a physisorption adsorption mechanism.

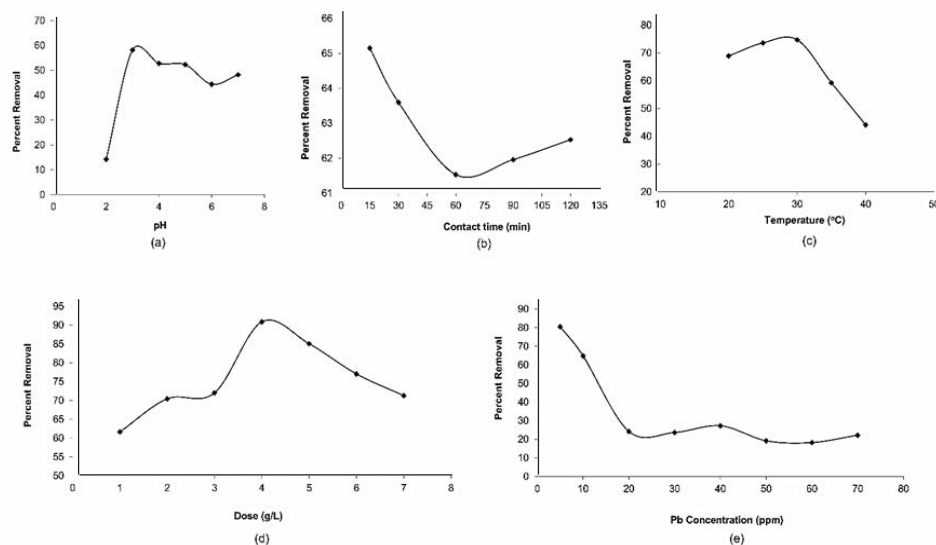


Fig. 5. Effect of (a) pH, (b) contact time, (c) temperature, (d) dose, and (e) metal concentration on Pb (II) adsorption on LAC/CMC/ECH composite

Table 2: Parameter estimates of the different isotherm models

Isotherm Model	Parameter	Estimated Value
Langmuir ($R^2=0.585$)	Q_o	2.245
	k_L (L/mg)	0.806
	R_L	0.166
Freundlich ($R^2=0.952$)	$1/n$	0.242
	k_f (mg/g)	1.088
Temkin ($R^2=0.952$)	A_T (L/mg)	11.840
	b_T (kJ/mol)	5.795
	B	0.428
Dubinin-Radushkevich ($R^2=0.971$)	q_s (mg/g)	0.007
	K_{ad} (mol ² /J ²)	2.0×10^{-6}
	E (kJ/mol)	0.500

Adsorption kinetics

Among the four identified kinetic equations, the pseudo-second order model best described the adsorption process ($R^2=0.998$). According to the pseudo-second order model, although physisorption is the mechanism of

adsorption on the adsorbent surface, the adsorption process is rate-limited by chemisorption^{32,33}. Furthermore, this supports the assumption that the adsorption process follows the D. R isotherm which describes the adsorption process to be physisorption. The pseudo-second order model is applicable in the kinetic studies of heavy metals and dyes sorption^{20,21,33,34}.

Efficiency experiment

The adsorption efficiency of commercial AC, LAC, CMC, LAC/CMC, and LAC/CMC/ECH towards Pb (II), under the optimized parameters, were compared. The prepared adsorbent exhibited the highest percent removal (72.61%) which suggests that LAC/CMC/ECH is a better adsorbent (Figure 6).

Wastewater analysis

The wastewater sample as detected by AAS contained various metallic substances aside from Pb(II) (Table 3). In addition, Cu(II) was also determined, however it was below the detection limit

of the instrument. LAC/CMC/ECH adsorbent was used for the Pb (II) uptake in the three solution systems (Fig. 7). The adsorbent exhibited commendable percent removal of dye and Pb(II) from methylene blue and Pb(II) aqueous solutions, respectively. However, the percent removal of Pb(II) in the wastewater sample is relatively low. This can be attributed to the presence of other substances in the wastewater sample that may interfere with the adsorption process.

Table 3: Heavy metals identified in the wastewater sample

Metal	Average Concentration (ppm)
Lead	1.138
Cadmium	0.085
Magnesium	2.124

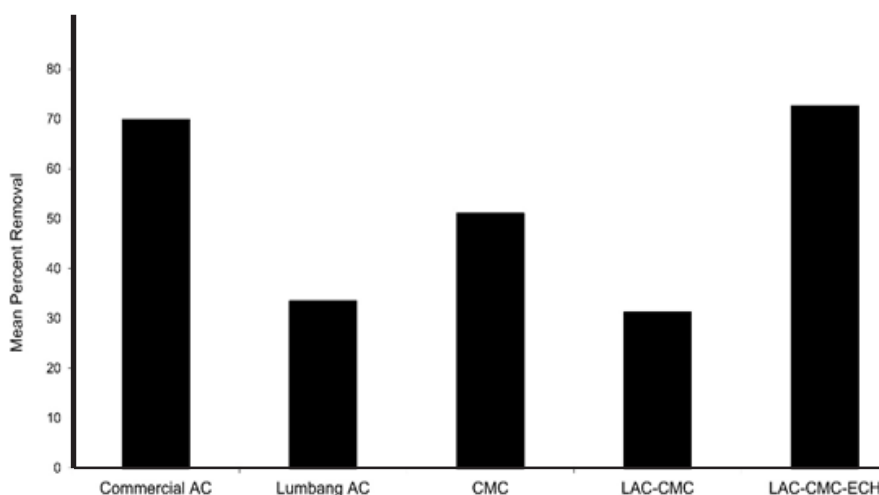


Fig. 6. Comparison of the percent removal of commercial AC, lumbang AC, CMC, LAC/CMC, and LAC/CMC/ECH

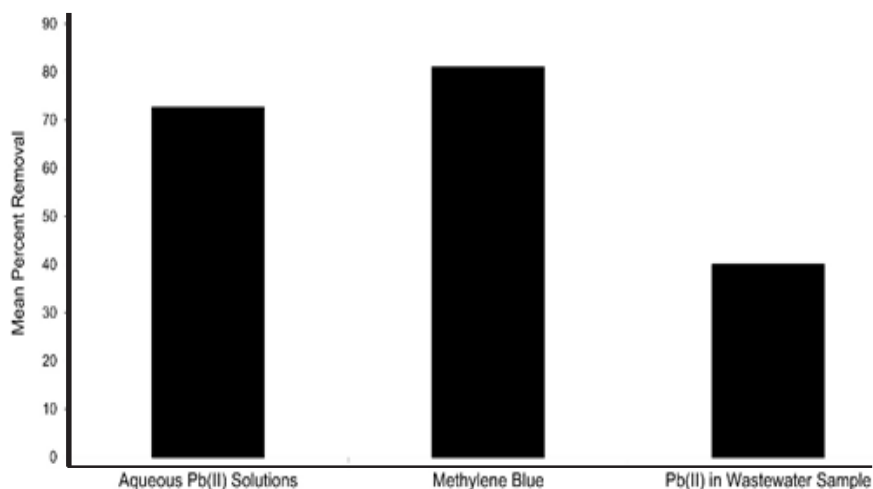


Fig. 7. Comparison of the percent removal of Pb (II) in aqueous solutions, methylene blue, and wastewater sample under optimum conditions

CONCLUSION

A low-cost activated carbon was successfully prepared and used to synthesize the LAC/CMC/ECH hydrogel adsorbent. The adsorbent was characterized using bulk density, proximate analysis, DSC, FT-IR spectroscopy, and SEM. With the optimized parameters for adsorption: pH 3 for 15 min. at 30 °C with 4 g/L adsorbent and 5 ppm Pb (II) concentration, Pb (II) was removed at high percentages in both aqueous and methylene blue

solutions, and in wastewater samples. The adsorption process was best described by the Dubinin-Radushkevich isotherm and obeyed the pseudo-second order kinetic model.

ACKNOWLEDGMENT

This work was supported by the National Institutes of Health, University of the Philippines Manila [NIH 2015-017].

REFERENCES

1. Sekar, M.; Sakthi, V.; Rengaraj, S. Kinetics and equilibrium adsorption study of lead (II) onto activated carbon prepared from coconut shell. *Journal of Colloid and Interface Science.*, **2004**, *279*(2), 307-313.
2. Momèiloviæ, M.; Purenoviæ, M.; Bojijæ, A.; Zarubica, A.; Ranðeloviæ, M. Removal of lead (II) ions from aqueous solutions by adsorption onto pine cone activated carbon. *Desalination.*, **2011**, *276*(1), 53-59.
3. Igbokwe, P.K.; Nwabanne, J.T. Preparation of activated carbon from Nipa palm nut: Influence of preparation conditions. *Research Journal of Chemical Sciences.*, **2011**.
4. Hu Z.; Srinivasan, M.P. Preparation of high-surface-area activated carbons from coconut shell. *Microporous and Mesoporous Materials.*, **1999**, *27*(1), 11-18.
5. Garcýa, A.I.; Otero, M.; Rozada, F.; Calvo, L.F.; Moran, A. Kinetic and equilibrium modelling of the methylene blue removal from solution by adsorbent materials produced from sewage sludges. *Biochemical Engineering Journal.*, **2003**, *15*(1), 59-68.
6. Markova, K.; Shopova, N.; Minkova, V. Evaluation of the thermochemical changes in agricultural by-products and in the carbon adsorbents obtained from them. *Journal of Thermal Analysis.*, **1997**, *48*(2), 309-320.
7. Cobb, A.; Warms, M.; Maurer, E.P.; Chiesa, S. Low-tech coconut shell activated charcoal production. *International Journal for Service Learning in Engineering, Humanitarian Engineering and Social Entrepreneurship.*, **2012**, *7*(1), 93-104.
8. Acharya, J.; Sahu, J.N.; Mohanty, C.R.; Meikap, B.C. Removal of lead (II) from wastewater by activated carbon developed from Tamarind wood by zinc chloride activation. *Chemical Engineering Journal.*, **2009**, *149*(1), 249-262.
9. Gumus, R.H.; Okpeku, I. Production of activated carbon and characterization from snail shell waste (*Helix pomatia*). *Advances in Chemical Engineering and Science.*, **2014**, *5*(1), 51.
10. Imamoglu, M.; Tekir, O. Removal of copper (II) and lead (II) ions from aqueous solutions by adsorption on activated carbon from a new precursor hazelnut husks. *Desalination.*, **2008**, *228*(1), 108-113.
11. Auta, M.; Hameed, B.H. Coalesced chitosan activated carbon composite for batch and fixed-bed adsorption of cationic and anionic dyes. *Colloids and Surfaces B: Biointerfaces.*, **2013**, *105*, 199-206.
12. Wei, M.; Kim, S.; Song, M.H.; Bediako, J.K.; Yun, Y.S. Carboxymethyl cellulose fiber as a fast binding and biodegradable adsorbent of heavy metals. *Journal of the Taiwan Institute of Chemical Engineers.*, **2015**.
13. Chen, C.Y.; Yang, C. Y.; Chen, A.H. Biosorption of Cu (II), Zn (II), Ni (II) and Pb (II) ions by cross-linked metal-imprinted chitosans with epichlorohydrin. *Journal of Environmental Management.*, **2011**, *92*(3), 796-802.
14. Qiu, J.; Xu, L.; Peng, J.; Zhai, M.; Zhao, L.; Li, J.; Wei, G. Effect of activated carbon on the properties of carboxymethylcellulose/activated carbon hybrid hydrogels synthesized by c-radiation technique. *Carbohydrate Polymers.*, **2007**, *70*, 236-242.
15. Yang, S.; Fu, S.; Liu, H.; Zhou, Y.; Li, X. Hydrogel beads based on carboxymethyl cellulose for removal heavy metal ions. *Journal of Applied Polymer Science.*, **2011**,

- 119(2), 1204-1210.
16. Gedam, A.H.; Dongreb, R.S. Activated carbon from *Luffa cylindrica* doped chitosan for mitigation of lead(II) from an aqueous solution. *RSC Adv.*, **2016**, *6*, 22639–22652.
 17. Dada, A.O.; Olalekan, A. P.; Olatunya, A. M.; Dada, O. Langmuir, Freundlich, Temkin and Dubinin–Radushkevich isotherms studies of equilibrium sorption of Zn²⁺ unto phosphoric acid modified rice husk. *Journal of Applied Chemistry.*, **2012**, *3*(1), 38-45.
 18. Liu, Q.S.; Zheng, T.; Wang, P.; Jiang, J.P.; Li, N. Adsorption isotherm, kinetic and mechanism studies of some substituted phenols on activated carbon fibers. *Chemical Engineering Journal.*, **2010**, *157*(2), 348-356.
 19. Auta, M.; Hameed, B.H. Preparation of waste tea activated carbon using potassium acetate as an activating agent for adsorption of Acid Blue 25 dye. *Chemical Engineering Journal.*, **2011**, *171*(2), 502-509.
 20. Sumalapao, D.E.P.; Distor, J.R.; Ditan, I.D.; Domingo, N.T.S.; Dy, L.F.; Villarante, N.R. Biosorption kinetic models on the removal of congo red onto unripe calamansi (*Citrus microcarpa*) peels. *Orient. J. Chem.*, **2016**, *32*(6), 2889-2900.
 21. Villarante, N.R.; Bautista, A.P.R.; Sumalapao, D.E.P. Batch adsorption study and kinetic profile of Cr(VI) using lumbang (*Aleurites moluccana*)-derived activated carbon-chitosan composite crosslinked with epichlorohydrin. *Orient. J. Chem.*, **2017**, *33*(3), 1111-1119.
 22. Singh, A.; Sharma, R.K.; Agrawal, M.; Marshall, F.M. Health risk assessment of heavy metals via dietary intake of foodstuffs from the wastewater irrigated site of a dry tropical area of India. *Food and Chemical Toxicology.*, **2010**, *48*(2), 611-619.
 23. Yan, H.; Zhang, W.; Kan, X.; Dong, L.; Jiang, Z.; Li, H.; Cheng, R. Sorption of methylene blue by carboxymethyl cellulose and reuse process in a secondary sorption. *Colloids and Surfaces A: Physicochemical and Engineering Aspects.*, **2011**, *380*(1), 143-151.
 24. Han, X.; Ghoroi, C.; To, D.; Chen, Y.; Davé, R. Simultaneous micronization and surface modification for improvement of flow and dissolution of drug particles. *International Journal of Pharmaceutics.*, **2011**, *415*(1), 185-195.
 25. Dhawade, P.P.; Jagtap, R. N. Characterization of the glass transition temperature of chitosan and its oligomers by temperature modulated differential scanning calorimetry. *Adv Appl Sci Res.*, **2012**, *3*(3), 1372-1382.
 26. Liu, Y.; Wang, W.; Wang, A. Adsorption of lead ions from aqueous solution by using carboxymethyl cellulose-g-poly (acrylic acid)/attapulgite hydrogel composites. *Desalination.*, **2010**, *259*(1), 258-264.
 27. Soundarajan, M.; Gomathi, T.; Sudha, P.N. Understanding the adsorption efficiency of chitosan coated carbon on heavy metal removal. *International Journal of Scientific and Research Publication.*, **2013**, *3*(1), 1-10.
 28. Akpomie, K.G.; Dawodu, F.A.; Adebowale, K.O. Mechanism on the sorption of heavy metals from binary-solution by a low-cost montmorillonite and its desorption potential. *Alexandria Engineering Journal.*, **2015**, *54*(3), 757-767.
 29. Krishna, B.S.; Murty, D.S.R.; Prakash, B.S.J. Thermodynamics of chromium(VI) anionic species sorption onto surfactant-modified montmorillonite clay. *J. Colloid Interf. Sci.*, **2000**, *229*, 230–236.
 30. Lin, S.H.; Juang, R.S. Heavy metal removal from water by sorption using surfactant-modified montmorillonite. *J. Hazard. Mater. B.* **2002**, *92*, 315–326.
 31. Wang, C.C.; Juang, L.C.; Lee, C.K.; Hsua, T.C.; Leeb, J.F.; Chaob, H.P. Effects of exchanged surfactant cations on the pore structure and adsorption characteristics of montmorillonite. *J. Colloid Interf. Sci.*, **2004**, *280*, 27–35.
 32. Robati, D. Pseudo-second-order kinetic equations for modeling adsorption systems for removal of lead ions using multi-walled carbon nanotube. *Journal of Nanostructure in Chemistry.*, **2013**, *3*(1), 1-6.
 33. Bautista, A.P.R.; Sumalapao, D.E.P.; Villarante, N.R. Synthesis and characterization of epichlorohydrin-crosslinked lumbang (*Aleurites moluccana*)-derived activated carbon chitosan composite as Cr(VI) bioadsorbent. *Annual Research & Review in Biology.*, **2017**, *21*(1), 1-7.
 34. Kumar, K.V. Linear and non-linear regression analysis for the sorption kinetics of methylene blue onto activated carbon. *Journal of Hazardous Materials.*, **2006**, *137*(3), 1538-1544.